

A Characteristics Model for Electromagnetic Transient Analysis of Multiconductor Lines with Corona and Skin Effects

M. Dávila, J. L. Naredo, *Senior member IEEE*, P. Moreno, *IEEE M*

Abstract: This paper describes a multiconductor line model which includes Corona and Frequency Dependence Effects. It is based on the method of characteristics from the theory of partial differential equations and it is intended for electromagnetic transient analysis. One of the major features of this model is that it fully accounts for the nonlinear properties of the propagation line modes in a rigorous manner. The proposed model is applied in the simulation of a field experiment. These results show a good agreement with the corresponding field measurements.

Keywords: Electromagnetic Transients, Transmission Lines, Corona Effect, Frequency dependence.

I INTRODUCTION

IT is well known that overvoltage waves on overhead conductors are attenuated and distorted by skin and corona effects. In most cases the distortion caused by corona on propagating surges is much more pronounced than the one caused by skin effect; nevertheless, being able to perform a rigorous analysis of transients under both effects, corona and skin, is has been deemed as here highly important.

Several technical papers dealing with the electromagnetic transient analysis of lines with corona have been published. Most of these focus on the single phase case. References [1] to [6] are a partial list of these papers. References [3] and [6] include frequency dependence. On the other hand references [7], [8] and [9] deal with the transient analysis of multiconductor lines with corona.

In this paper, a model for multiconductor lines with corona previously reported in reference [10] is extended to include both the frequency dependence of the line parameters and the corona effect. This model is based on the method of characteristics from the theory of Partial Differential Equations (PDEs) and recursive convolution techniques are used to include frequency dependence. Two very important

features of the model being proposed here is that it takes into account that propagation line modes are functions of the line voltages, and that the propagating modes do not superpose in the usual linear manner.

For the validation of the proposed model, a field experiment performed by Wagner, *et al.*, [11] has been used. This experiment has been chosen because it contains a complete description of the experimental variables and conditions relevant for computer simulations. In addition, for this experiment waveforms were registered at various points along the transmission line. These experimental waveforms are available for the excited conductor as well as for the unenergized phases. It is considered here that the reproduction of the induced waveforms constitutes the most stringent test for the new model.

II MULTICONDUCTOR DISPERSIVE LINE MODEL

The Telegrapher's equations for multiconductor lines with frequency dependent parameters are [12,15]:

$$\frac{\partial \mathbf{v}}{\partial \mathbf{x}} + \mathbf{L}_G \frac{\partial \mathbf{i}}{\partial t} + \frac{\partial}{\partial t} \int_0^t \mathbf{r}'(t-\tau) \mathbf{i}(\tau) d\tau = \mathbf{0} \quad (1a)$$

$$\frac{\partial \mathbf{i}}{\partial \mathbf{x}} + \mathbf{C} \frac{\partial \mathbf{v}}{\partial t} = \mathbf{0}, \quad (1b)$$

where \mathbf{L}_G is the geometric inductance matrix of the line, \mathbf{C} is the capacitance matrix of the line and $\mathbf{r}'(t)$ is the matrix of transient series resistances of the line. To include corona effect, the matrix \mathbf{C} elements can be functions of the coronating conductor voltages, that is, of the elements of vector \mathbf{v} . This is accomplished as described in references [13],[14] and [10].

Frequency dependence, or skin effect, is accounted for in equation (1a) through the term involving the convolution between the transient resistances $\mathbf{r}'(t)$ and the line currents $\mathbf{i}(t)$. The transient resistance $\mathbf{r}'(t)$ has the following limits [12]:

$$\lim_{t \rightarrow \infty} \mathbf{r}'(t) = \text{diag}\{R_{dc,1}, R_{dc,2}, \dots, R_{dc,n}\} \quad (2a)$$

$$\lim_{t \rightarrow 0} \mathbf{r}'(t) = \text{diag}\{\infty, \infty, \dots, \infty\} \quad (2b)$$

where $R_{dc,q}$, $q = 1, 2, \dots, n$, is the DC resistance of q -th conductor, and $(\infty)_{n \times n}$ is an $n \times n$ square matrix whose elements are infinite. In the Laplace domain the image of $\mathbf{r}'(t)$ is $\mathbf{R}'(s)$ given by [12]:

Marisol Dávila gratefully acknowledges scholarships provision by the Universidad de Los Andes, Venezuela, to pursue post-graduate studies. M.Davila, J. L. Naredo and P. Moreno are with the Cinvestav, Guadalajara. Prol. López Mateos Sur 590, Guadalajara Jalisco-México.45090. (mdavila@gdl.cinvestav.mx, jlnaredo@gdl.cinvestav.mx, pmoreno@gdl.cinvestav.mx)

Presented at the International Conference on Power Systems Transients (IPST'05) in Montreal, Canada on June 19-23, 2005. Paper No. IPST05- # 056

$$\mathbf{R}'(s) = [\mathbf{Z}_g(s) + \mathbf{Z}_c(s)]/s \quad (3)$$

$\mathbf{R}'(s)$ is a symmetric matrix and each one of its elements is a transcendental function of s :

$$\mathbf{R}'(s) = \mathbf{k}_\infty + \mathbf{k}_o/s + \mathbf{H}(s) \quad (4)$$

Here \mathbf{k}_o is the matrix of residues of $\mathbf{R}'(s)$ at $s=\infty$, \mathbf{k}_∞ is its residues matrix at $s=0$ and the elements of $\mathbf{H}(s)$ are approximated here by rational functions of s as follows:

$$\mathbf{H}(s) = \sum_{j=1}^N \frac{\mathbf{k}_j}{s + p_j}, \quad (5)$$

here N is the order of the fit and \mathbf{k}_j ($i=1, \dots, N$) is the residue matrix of $\mathbf{H}(s)$ at pole $s = p_j$. The N poles p_1, p_2, \dots, p_N are obtained here through the vector fitting technique [17]. It follows from (4) and (5) that the approximate time domain image of $\mathbf{R}'(s)$ is:

$$\mathbf{r}'(t) \cong \mathbf{k}_o u(t) + \mathbf{k}_\infty \delta(t) + \mathbf{h}(t) \quad (7)$$

where $\delta(t)$ is the Dirac delta function, $u(t)$ is the unit step function and

$$\mathbf{h}(t) = u(t) \sum_{j=1}^N \mathbf{k}_j e^{-p_j t}. \quad (8)$$

On applying (7) in (1a) one obtains:

$$\frac{\partial \mathbf{v}}{\partial t} + \mathbf{D} \frac{\partial \mathbf{i}}{\partial t} + \mathbf{R}_{dc} \mathbf{i} + \frac{\partial}{\partial t} \int_0^t \mathbf{h}(t-\tau) \mathbf{i}(\tau) d\tau = \mathbf{0} \quad (9)$$

where

$$\mathbf{D} = \mathbf{k}_\infty + \mathbf{L}_G \quad (10)$$

Now, the Leibnitz rule for differentiating an integral is applied to (9) [15], thus obtaining:

$$\frac{\partial}{\partial t} \int_0^t \mathbf{h}(t-\tau) \mathbf{i}(\tau) d\tau = \mathbf{h}(0) \mathbf{i}(t) + \int_0^t \mathbf{h}'(t-\tau) \mathbf{i}(\tau) d\tau \quad (11)$$

Here $\mathbf{h}'(t)$ denotes the time derivative of $\mathbf{h}(t)$. It follows from (8) that

$$\mathbf{h}(0) = \sum_{j=1}^N \mathbf{k}_j \quad (12)$$

and

$$\mathbf{h}'(t) = -\sum_{j=1}^N \mathbf{k}_j p_j e^{-p_j t} \quad (13)$$

Expression (13) is next introduced in (9):

$$\frac{\partial \mathbf{v}}{\partial x} + \mathbf{D} \frac{\partial \mathbf{i}}{\partial t} + \mathbf{R}_X \mathbf{i} + \int_0^t \mathbf{h}'(t-\tau) \mathbf{i}(\tau) d\tau = \mathbf{0}, \quad (14)$$

where:

$$\mathbf{R}_X = \mathbf{R}_{dc} + \mathbf{h}(0) \quad (15)$$

From all the above, Telegrapher equation (1a) becomes:

$$\frac{\partial \mathbf{v}}{\partial x} + \mathbf{D} \frac{\partial \mathbf{i}}{\partial t} + \mathbf{R}_X \mathbf{i} + \mathcal{G} = \mathbf{0} \quad (16)$$

with

$$\mathcal{G} = \int_0^t \mathbf{h}'(t-\tau) \mathbf{i}(\tau) d\tau \quad (17)$$

III CORONA REPRESENTATION FOR MULTICONDUCTOR LINES

In a very general sense, it can be said that the corona effect appears when the magnitude of an electric field around a line conductor becomes greater than the dielectric strength of the air. The air molecules near the conductor break into ions, and the conductor capacitance ceases to be constant and linear. Usually, for the transient analysis of lines, the corona effect is included by making the capacitance parameter a function of the line voltage. In most cases these functions are derived from experimental Q-V curves [3].

The Q-V curves, as well as most of the available corona models, are intended for single phase lines. An extension of the Q-V curves to the multiconductor line case was first proposed in [13] and has been adopted here. Further details of this extension are available in [10] and [14], and a brief description of it is provided next.

Consider an aerial line with n parallel horizontal conductors above the ground plane as illustrate in figure 1. The relationship between the vectors of phase voltages and of conductor charge densities is given through the matrix of Maxwell potential coefficients as follows:

$$\mathbf{v} = \mathbf{P} \boldsymbol{\rho} \quad (18)$$

Or, in an explicit form:

$$\begin{bmatrix} v_1 \\ v_2 \\ v_i \\ \vdots \\ v_n \end{bmatrix} = \begin{bmatrix} P_{11} & P_{12} & P_{1i} & \cdots & P_{1n} \\ P_{21} & P_{22} & P_{2i} & \cdots & P_{2n} \\ P_{i1} & P_{i2} & P_{ii} & \cdots & P_{in} \\ \vdots & \vdots & \vdots & \ddots & \vdots \\ P_{n1} & P_{n2} & P_{ni} & \cdots & P_{nn} \end{bmatrix} \begin{bmatrix} \rho_1 \\ \rho_2 \\ \rho_i \\ \vdots \\ \rho_n \end{bmatrix} \quad (19)$$

The self potential coefficients have the following form:

$$P_{ii} = \frac{1}{2\pi\epsilon_o} \ln \left(\frac{2h_i}{r_i} \right) \quad i=1,2,\dots,n \quad (20)$$

where h_i and r_i are corresponding height and radius of the i -th conductor. The mutual potential coefficients are given by:

$$P_{ij} = \frac{1}{2\pi\epsilon_o} \ln \left(\frac{D_{ij}}{d_{ij}} \right) \quad i,j=1,2,\dots,n; i \neq j \quad (21)$$

where D_{ij} is the distance between conductor " i " and the image of conductor " j ", while d_{ij} is the actual distance between conductors " i " and " j ".

Now consider that conductor " i " in figure 1 enters in corona. If one can assume that the spatial corona charge is uniformly distributed inside a cylindrical shell around the conductor, and that the center of charge still is at the height h_i , only the self potential coefficients P_{ii} at expression (19) is modified by the corona and, in fact, conductor radius r_i must be replaced by a fictitious one dependent on voltage v_i if one still wants to preserve expression 20. If in addition to conductor " i " other conductors enter in corona, only their corresponding self potential coefficients are affected becoming each a function of its own voltage. It can thus be stated that an extension of the Q-V curve concept to the multiconductor line case is provided by expressions 19, 20 and 21 when the radii r_1, r_2, \dots, r_n , are allowed to depend each on its corresponding voltage v_1, v_2, \dots or v_n .

Let now, expressions 18 (or 19) be inverted:

$$\rho = \mathbf{C}' \mathbf{v} \quad (22)$$

Matrix $\mathbf{C}' = \mathbf{P}^{-1}$ has the dimensions of capacitance in per unit of length. If the i -th conductor is in corona clearly, by the process of inversion, all the elements of \mathbf{C}' are functions of v_i . If several conductors are simultaneously in corona, matrix \mathbf{C}' obtained inverting \mathbf{P} will be a function of all the coronating conductor voltages. It should be mentioned at this point that

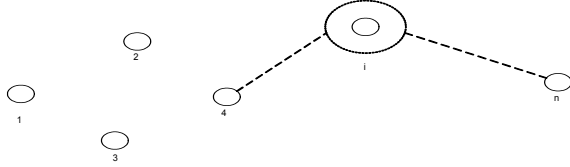


Fig.1. Multiconductor Line

the matrix \mathbf{C}' so obtained is not yet the line capacitance parameter \mathbf{C} required in expression (1b). A further consideration has still to be made regarding the law of conservation of charge:

$$-\frac{\partial \mathbf{i}}{\partial x} = \frac{\partial \rho}{\partial t}, \quad (23)$$

From (22):

$$-\frac{\partial \mathbf{i}}{\partial x} = \frac{\partial (\mathbf{C}' \mathbf{v})}{\partial t} \quad (24)$$

On applying the chain rule:

$$-\frac{\partial \mathbf{i}}{\partial x} = \frac{\partial (\mathbf{C}' \mathbf{v})}{\partial \mathbf{v}} \frac{\partial \mathbf{v}}{\partial t} \quad (25)$$

and

$$-\frac{\partial \mathbf{i}}{\partial x} = (\mathbf{C}' + \mathbf{C}'') \frac{\partial \mathbf{v}}{\partial t} \quad (26)$$

In this last expression, \mathbf{C}'' is an $n \times n$ matrix whose elements have the following form [13,14]:

$$C''_{ij} = \sum_{j=1}^n \frac{\partial C'_{ij}}{\partial v_j} v_j \quad (27)$$

IV NONLINEAR AND DISPERSIVE LINE MODEL IN CHARACTERISTIC COORDINATES

Let (16) and (1b) be grouped as follows [16]:

$$\frac{\partial \mathbf{U}}{\partial t} + \mathbf{A} \frac{\partial \mathbf{U}}{\partial x} + \mathbf{B} \mathbf{U} + \mathbf{F} = \mathbf{0} \quad (28a)$$

where

$$\mathbf{U} = \begin{bmatrix} \mathbf{v} \\ \mathbf{i} \end{bmatrix}, \quad (28b)$$

$$\mathbf{A} = \begin{bmatrix} \mathbf{0} & \mathbf{C}^{-1} \\ \mathbf{D}^{-1} & \mathbf{0} \end{bmatrix}, \quad (28c)$$

$$\mathbf{B} = \begin{bmatrix} \mathbf{0} & \mathbf{0} \\ \mathbf{0} & \mathbf{D}^{-1} \mathbf{R}_x \end{bmatrix} \quad (28d)$$

and

$$\mathbf{F} = \begin{bmatrix} \mathbf{0} \\ \mathbf{D}^{-1} \rho \end{bmatrix} \quad (28e)$$

Consider also the following factorization of \mathbf{A} in its eigenvalue and eigenvector matrices [16]:

$$\mathbf{A} = \mathbf{E}_L \mathbf{\Gamma} \mathbf{E}_L^{-1} \quad (29)$$

where \mathbf{E}_L is the matrix of left eigenvectors and $\mathbf{\Gamma}$ is the matrix of eigenvalues. It can be further shown that the latter matrix always is diagonal [16].

Now, equation (28) is left-multiplied by \mathbf{E}_L :

$$\mathbf{E}_L \frac{\partial \mathbf{U}}{\partial t} + \mathbf{E}_L \mathbf{A} \frac{\partial \mathbf{U}}{\partial x} + \mathbf{E}_L \mathbf{B} \mathbf{U} + \mathbf{E}_L \mathbf{F} = \mathbf{0} \quad (30)$$

It follows from (29) that:

$$\mathbf{E}_L \frac{\partial \mathbf{U}}{\partial t} + \mathbf{\Gamma} \mathbf{E}_L \frac{\partial \mathbf{U}}{\partial x} + \mathbf{E}_L \mathbf{B} \mathbf{U} + \mathbf{E}_L \mathbf{F} = \mathbf{0} \quad (31)$$

This last expression consists of $2n$ scalar equations of the form:

$$\mathbf{E}_{Lj} \left(\frac{\partial \mathbf{U}}{\partial t} + \gamma_j \frac{\partial \mathbf{U}}{\partial x} \right) + \mathbf{E}_{Lj} \mathbf{B} \mathbf{U} + \mathbf{E}_{Lj} \mathbf{F} = \mathbf{0} \quad (32)$$

where \mathbf{E}_{Lj} denotes the j -th row of matrix \mathbf{E}_L or the j -th left eigenvector of \mathbf{A} , and γ_j is the j -th eigenvalue of \mathbf{A} . The term $\left(\frac{\partial \mathbf{U}}{\partial t} + \gamma_j \frac{\partial \mathbf{U}}{\partial x} \right)$ in (32) corresponds to the total derivative of \mathbf{U} with respect to t , provided this derivative is evaluated along the trajectory defined by:

$$dx/dt = \gamma_j \quad (33)$$

The trajectories in the X - T plane defined by equations of the form (33) are said to be the characteristics of PDE system (28). Along the characteristic curve (33), expression (32) becomes thus:

$$\mathbf{E}_{Lj} \left(\frac{d\mathbf{U}}{dt} \right) + \mathbf{E}_{Lj} \mathbf{B} \mathbf{U} + \mathbf{E}_{Lj} \mathbf{F} = \mathbf{0} \quad (34)$$

V NUMERICAL SOLUTION OF LINE EQUATIONS

Figure 2 illustrates the numerical solution of the $2n$ equations of the form (34). Point G is located on the line $t = T + \Delta t$. Along with this point included are the plots of the $2n$ characteristics passing through it. The figure also illustrates the regular grid of finite differences used in the numerical solution of the $2n$ equations. Suppose now that solution values of \mathbf{U} are known at the points D , E and F located on line $t = T$ and that these solutions are to be extended to point G . Note in the figure that the $2n$ characteristics passing through G will intersect the line $t = T$ at points D_1 , D_2 , ..., and D_{2n} which, in general, will not coincide with D , E and F . Each one of the $2n$ equations of the form (34) are integrated between $t = T$ and $t = T + \Delta t$ as follows through the mean value theorem:

$$\tilde{\mathbf{E}}_{Lj} (\mathbf{U}^G - \mathbf{U}^{Dj}) + \Delta t \tilde{\mathbf{E}}_{Lj} \mathbf{B} \tilde{\mathbf{U}} + \Delta t \tilde{\mathbf{E}}_{Lj} \tilde{\mathbf{F}} = \mathbf{0} \quad (35)$$

where the tilde denotes mean values. A numerical approximation of (35) is obtained by replacing each mean value by its two end point average:

$$\tilde{\mathbf{E}}_{Lj} \approx (\mathbf{E}_{Lj}^G + \mathbf{E}_{Lj}^{Dj})/2 \quad (36)$$

$$\tilde{\mathbf{U}} \approx (\mathbf{U}^G + \mathbf{U}^{Dj})/2 \quad (37)$$

and

$$\tilde{\mathbf{F}} = (\mathbf{F}^G + \mathbf{F}^{Dj})/2 \quad (38)$$

Note in equations (35), (36), (37) and (38) that the values of \mathbf{U} , \mathbf{E}_{Lj} and \mathbf{F} are required at point D_j , where the j -th characteristic defined by (33) intersects the horizontal line $t = T$. Assume momentarily that the coordinates of D_j are established. The required values at point D_j can thus be obtained from known data at points D , E and F through quadratic interpolations:

$$\mathbf{E}_{Lj}^{Dj} = \alpha_{1j}\mathbf{E}_{Lj}^D + \alpha_{2j}\mathbf{E}_{Lj}^E + \alpha_{3j}\mathbf{E}_{Lj}^F, \quad (39a)$$

$$\mathbf{U}_j^{Dj} = \alpha_{1j}\mathbf{U}^D + \alpha_{2j}\mathbf{U}^E + \alpha_{3j}\mathbf{U}^F \quad (39b)$$

and

$$\mathbf{F}_j^{Dj} = \alpha_{1j}\mathbf{F}^D + \alpha_{2j}\mathbf{F}^E + \alpha_{3j}\mathbf{F}^F \quad (39c)$$

where α_{1j} , α_{2j} and α_{3j} are the corresponding interpolation coefficients:

$$\alpha_{1j} = (r_j)^2/2 - (r_j)/2, \quad (40a)$$

$$\alpha_{2j} = 1 - (r_j)^2, \quad (40b)$$

$$\alpha_{3j} = (r_j)^2/2 + (r_j)/2 \quad (40c)$$

and

$$r_j = \bar{\gamma}_j(\Delta t / \Delta x) \quad (40d)$$

In the last expression $\bar{\gamma}_j$ represents the mean value of γ_j along a segment of the j -th characteristic comprised between $t = T$ and $t = T + \Delta t$. This mean value can be further approximated as follows by its two end point average:

$$\bar{\gamma}_j \approx (\gamma_j^G + \gamma_j^{Dj})/2. \quad (41)$$

while γ_j^{Dj} is given by:

$$\gamma_j^{Dj} = \alpha_{1j}\gamma_j^D + \alpha_{2j}\gamma_j^E + \alpha_{3j}\gamma_j^F \quad (42)$$

If the frequency dependence effects of the line were not to be accounted for, the numerical process described so far would be sufficient for simulating transients propagating on a multiconductor line with corona through iterations. This has been done already in references [10] and [13]. As frequency dependence is brought into consideration, one should realize that the term \mathbf{F}^G involves vector \mathfrak{G}_G which in turn is generated by n convolutions, according to (17). Due to the fact that $h'(t)$ is approximated in (8) by a sum of exponential functions, the required convolutions can be evaluated recursively. In broad terms this means for instance that \mathfrak{G}_G can be obtained by simply updating the value of \mathfrak{G} previously determined one time step Δt before (*i.e.*, \mathfrak{G}_E).

To explain the convolutional term update, consider the following decomposition of vector \mathfrak{G}_G :

$$\mathfrak{G}_G = \sum_{j=1}^N \mathfrak{G}_{G,j}, \quad (43)$$

where, according to (13):

$$\mathfrak{G}_{G,j} = -\mathbf{k}_j p_j \int_0^t e^{-p_j(t-\tau)} \mathbf{i}(\tau) d\tau \quad (44)$$

Assume now that vector \mathfrak{G}_E and its N components $\mathfrak{G}_{E,1}$, $\mathfrak{G}_{E,2}$, ..., $\mathfrak{G}_{E,N}$ are known from time $t=T$. Each one of the terms $\mathfrak{G}_{G,j}$

at the next instant of time $t=T+\Delta t$ is obtained through the following recursion [12]:

$$\mathfrak{G}_{G,j} = -\frac{1}{1+p_j\Delta t} \mathfrak{G}_{E,j} - \frac{\Delta t p_j \mathbf{k}_j}{1+p_j\Delta t} \mathbf{i}_G \quad (45)$$

By defining

$$\mathbf{K}_j' = -\frac{1}{1+p_j\Delta t} \mathfrak{G}_{E,j} \quad \text{and} \quad \mathbf{K}_j'' = -\frac{\Delta t p_j \mathbf{k}_j}{1+p_j\Delta t} \mathbf{i}_G,$$

expression (45) becomes:

$$\mathfrak{G}_{G,j} = \mathbf{K}_j' \mathfrak{G}_{E,j} + \mathbf{K}_j'' \mathbf{i}_G \quad (46)$$

It is clear that the first term of (46) is the history of convolution, and that the second one (*i.e.*, the update) includes the vector of unknown currents \mathbf{i}_G . On applying (46) in (43) one obtains:

$$\mathfrak{G}_G = \mathbf{K}_E + \mathbf{K}'' \mathbf{i}_G \quad (47a)$$

where

$$\mathbf{K}_E = \sum_{j=1}^N \mathbf{K}_j' \mathfrak{G}_{E,j} \quad (47b)$$

and

$$\mathbf{K}'' = \sum_{j=1}^N \mathbf{K}_j'' \quad (47c)$$

It thus follows from (28b), (28e), (47a), (47b) and (47c) that:

$$\mathbf{F}^G = \begin{bmatrix} \mathbf{0} \\ \mathbf{D}^{-1} \mathbf{K}_E \end{bmatrix} + \begin{bmatrix} \mathbf{0} & \mathbf{0} \\ \mathbf{0} & \mathbf{D}^{-1} \mathbf{K}'' \end{bmatrix} [\mathbf{U}^G] = \mathbf{F}^{GP} + \mathbf{F}^X \mathbf{U}^G \quad (48)$$

Let now (36), (37), (38) and (48) be applied in (35):

$$\begin{aligned} & (\mathbf{E}_{Lj}^G + \mathbf{E}_{Lj}^{Dj})(\mathbf{U}^G - \mathbf{U}^{Dj}) + \frac{\Delta t}{2} (\mathbf{E}_{Lj}^G + \mathbf{E}_{Lj}^{Dj}) \mathbf{B} (\mathbf{U}^G + \mathbf{U}^{Dj}) + \\ & \frac{\Delta t}{2} (\mathbf{E}_{Lj}^G + \mathbf{E}_{Lj}^{Dj}) (\mathbf{F}^{GP} + \mathbf{F}^X \mathbf{U}^G + \mathbf{F}^{Dj}) = \mathbf{0} \end{aligned} \quad (49)$$

Finally, after some algebraic manipulations, the following expression is obtained:

$$\begin{aligned} & (\mathbf{E}_{Lj}^G + \mathbf{E}_{Lj}^{Dj}) \mathbf{B}' \mathbf{U}^G = (\mathbf{E}_{Lj}^G + \mathbf{E}_{Lj}^{Dj}) \mathbf{B}'' \mathbf{U}^{Dj} - \\ & \frac{\Delta t}{2} (\mathbf{E}_{Lj}^G + \mathbf{E}_{Lj}^{Dj}) (\mathbf{F}^{GP} + \mathbf{F}^{Dj}) \end{aligned} \quad (50a)$$

where:

$$\mathbf{B}' = \mathbf{1} + (\Delta t/2) (\mathbf{B} + \mathbf{F}^X), \quad (50b)$$

$$\mathbf{B}'' = \mathbf{1} - (\Delta t/2) \mathbf{B} \quad (50c)$$

and $\mathbf{1}$ is the $2n \times 2n$ unit matrix.

Expression (50a) is a discrete version of (34). If the values of \mathbf{U} are known at points D , E and F , one can iterate the $2n$ equations of the form (50a) representing the multiconductor line being analyzed to determine the value of \mathbf{U} at point G , and so on. This iterative procedure has been amply described in references [5], [6], [10], [13] and [16].

VI SIMULATION OF A FIELD EXPERIMENT.

The above described method has been implemented in a digital computer program for simulating electromagnetic transients on multiconductor lines with corona and frequency dependence effects. This program now is applied in the simulation of a field experiment performed by Wagner, Gross and Lloyd in the 1950s [11]. There are several strong reasons

for choosing this experiment as benchmark. One of them is that this experiment is perhaps the most comprehensive one ever carried out. A second reason is that its report provides most details required to build up simulations. A third reason is that waveforms were registered at various points along the experimental line, as well as at all the phase conductors. This last feature is essential for testing multiconductor line models. Another good reason is that a large number of models for lines with corona have been tested with this experiment.

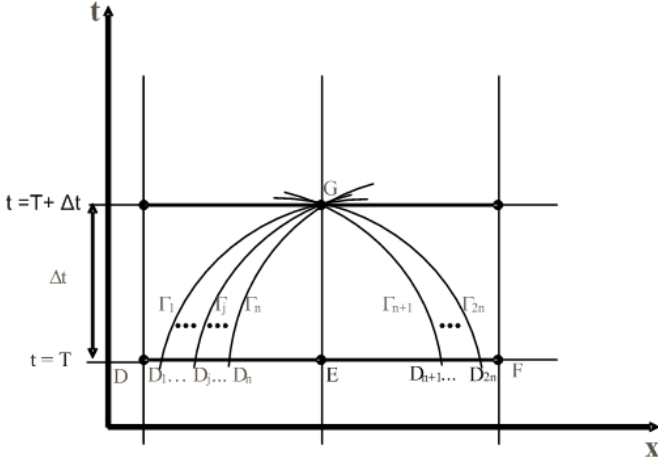


Fig. 2. Discretization mesh.

The abovementioned experiment consisted in the injection of a $1.56 \text{ MV}/0.35 \mu\text{s}/6 \mu\text{s}$ impulse at the beginning of a 2185 m long line. The actual line consisted of three ACSR conductors in horizontal layout with equal radii $r=2.54 \text{ cm}$ and a medium height at $h=18.9 \text{ m}$. The horizontal distance between adjacent conductors was $d=9.75 \text{ m}$. The impulse was injected at the beginning of the central conductor (phase “b”). Whereas the lateral conductors were left open, the center conductor was terminated in an impedance $Z_L=400 \Omega$. Figure 3 shows a diagram of the experiment layout. Figures 4a and 4b provide the waveforms measured at various points along the line. Figure 4a plots provide the voltage waveforms registered at the energized central phase. Figure 4b, on the other hand, provides the waveforms measured on one of the lateral phases which, because of the line symmetry, have to be equal.

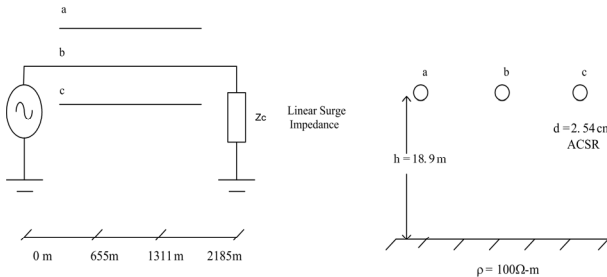


Fig. 3. Experimental line configuration.

For simulation purposes, the earth resistivity is assumed here at $\rho_g=100 \Omega\text{-m}$, and the corona inception voltage is determined at 450 kV by means of Peek’s formula [16]. The injected pulse is approximated by a double exponential. Figures 5a and 5b show the waveforms obtained with the method being proposed here. The simulations have been made

both, with and without frequency dependence. The plots in figure 5a should be compared with those of figure 4a, while the ones in figure 5b should be compared with those in figure 4b.

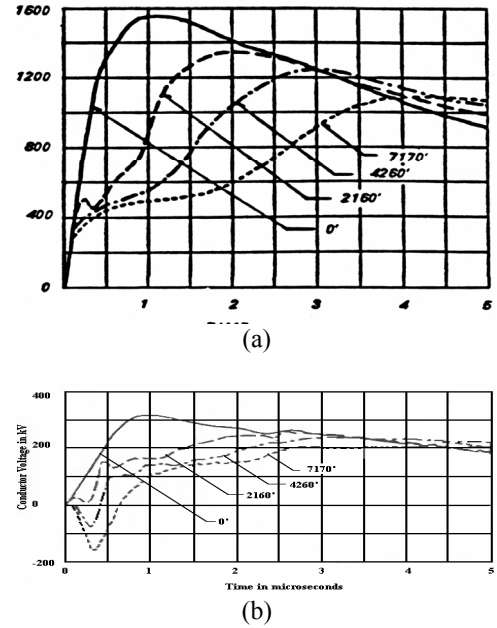


Fig. 4. Experimental results from Wagner, *et. al.*, a) Energized phase response. b) Induced waveforms

The comparisons between measured and simulated results are very encouraging. It can be observed that the simulations including frequency dependence and corona are closer to the experimental curves. These authors consider that the most stringent test for the line model being proposed is the reproduction of the induced waveforms. These authors believe also that for an even closer agreement between simulated and measured results, one should perhaps include in the line model the non uniform effects caused by the sagging of the conductors.

VII. CONCLUSIONS.

In this paper, a transmission line model based on the method of finite differences in characteristic coordinates has been presented. This model has been devised for analyzing electromagnetic transients on lines affected both, by corona and frequency dependence effects. The latter effects have been dealt with through rational fitting and recursive convolution techniques[17]. A distinctive feature of this model is that it accounts for the facts that line modes are dependent on voltage (*i.e.*, nonlinear) and that they do not superpose in the usual linear manner. The model has been applied in the reproduction of a field experiment by Wagner, *et al.*, [11]. Comparisons between experimentally measured and simulated waveforms are very encouraging. More over, it has been shown that a simulation including corona and frequency dependence yields results closer to experiments than a simulation including only corona effect. The performance attained by the proposed model has been deemed by these authors as a quite satisfactory one. It has been considered that for an even closer match with experimental results one should have to include

the line non uniform effects caused by the sagging of the aerial conductors.

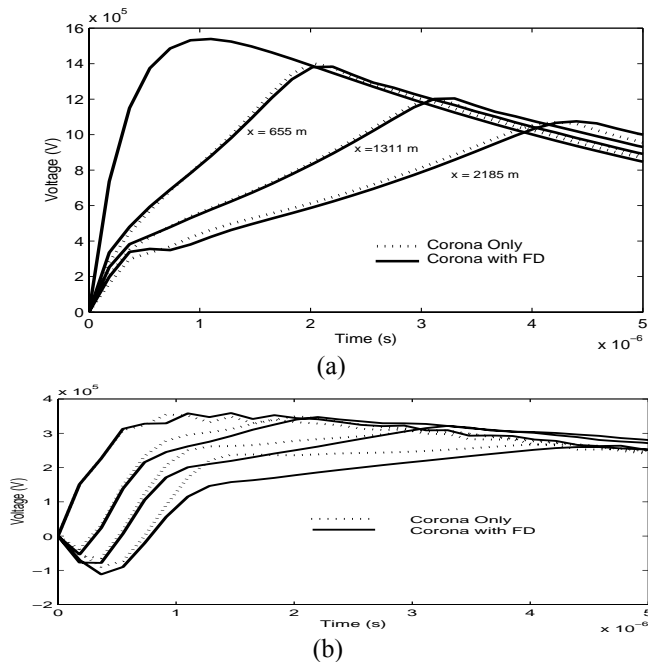


Fig. 5 Simulated results considering Corona Effect with and without frequency dependence. a) Energized phase response. b) Induced waveforms.

These authors admit that the complexity of the proposed model is very high. Nevertheless, once this model has been programmed for a digital computer, it can be easily used by third parties. Since Bergeron's method is a special case of the method of Characteristics, these authors do not foresee any major difficulty for implementing the proposed model in EMTP. These authors are currently engaged in applying the proposed model in the testing of more simple ones for simulating transients on multiconductor lines with corona.

Finally, it should be mentioned here that one major difficulty encountered by these authors in the development of the proposed model is the switching of matrix **A** modes as the voltages vary within the corona ranges. The techniques developed for linear lines do not solve this problem [18]. So far, an acceptable solution has been found for the case of three phase lines. A reliable solution to the more general case is still being sought.

VIII. REFERENCES

- [1] H. M. Kudyayn, C. H. Shih, "A Nonlinear Circuit Model for Transmission Lines in Corona", *IEEE/PES Summer Meeting*, July 13-18, 1980.
- [2] R. J. Harington, M. Afghahi, "Implementation of a Computer Model to Include the Effects of Corona in Transient Overvoltages Calculations". *IEEE PES 1982 Summer Meeting*, July 18-23, 1982.
- [3] C. Gary, A. Timotin, D. Cristecu, "Prediction of surge propagation influenced by corona and skin effect". *IEE Proceedings*, Vol.130, No.5. pp. 264-272, 1983.
- [4] S. Carneiro Jr. J. R. Martí, "Evaluation of Corona and Line Models in Electromagnetic Transients Simulations". *IEE Transactions on Power Delivery*, Vol. 6. No. 1, pp. 334-342, January, 1991.
- [5] J. L. Naredo, A. C. Soudack, J. R. Martí, "Simulation of transients on transmission lines with corona via the method of characteristics", *IEE Proceedings: Generation, Transmission and Distribution*. Vol. 142, No. 1, pp.81-87.

- [6] A. Ramírez, J. L. Naredo, P. Moreno, L. Guardado. "Electromagnetic transients in overhead lines considering frequency dependence and corona effect via the method of characteristics", *Electrical Power & Energy Systems*, 23 (2001), 179-188.
- [7] H. Wei-Gang, A. Semlyen, "Computation of Electromagnetic Transients on Three-Phase Transmission Lines with Corona and Frequency Dependent Parameters", *IEEE Trans. On Power Delivery*, Vol. PWRD-2, No. 3, pp. 887-898. July 1987.
- [8] M. Polojadff, M. Rioual, "Damping Model of Traveling Waves by Corona Effect along Extra High Voltage Three Phase Lines", *IEEE Paper 94 WM 042-2 PWRD*.
- [9] H. M. Barros, S. Carneiro Jr, R. M. Azevedo, "An Efficient Recursive Scheme for the Simulation of Overvoltages on Multiphase Systems Under Corona", *IEEE Trans. On Power Delivery*, Vol. 10, No. 3, pp. 1444-1452, July 1995.
- [10] M. Davila, J. L. Naredo, P. Moreno, J. A. Gutierrez, P. Gomez. "Analysis Transients on Multiconductor Lines with Corona", *IEEE/PES T&D 2004, Latin America, Sao Paulo, Brazil*. Nov, 2004.
- [11] C. F. Wagner, I. W. Gross, B. L. Lloyd, "High-Voltage Impulse Test on Transmission Lines", *AIEE Trans., PAS-73*, April 1954, 196-210.
- [12] Abner Ramirez, J. L. Naredo, Pablo Moreno, "Full Frequency Dependent Line Model for Electromagnetic Transient Simulation Including Lumped and Distributed Sources", *IEEE Transactions on Power Delivery*, Vol. 19, No. 1, pp. 292-299, January 2005.
- [13] J. L. Naredo, A. C. Soudack, J. R. Martí, "Transient Analysis of Single Phase and multiconductor Lines with Corona through the Method of Characteristics", *Proc. 11th Power System Computation Conference*, pp.1063-1069, Avignon, 1993.
- [14] M. T. Correia de Barros, "Identification of the Capacitance Coefficients of Multiphase Transmission Lines Exhibiting Corona Under Transient Conditions", *IEEE Transactions and Power Delivery*, Vol. 10, No. 3, pp. 1642-1648, 1995.
- [15] R. Radulet, Al. Timotin, A. Tugulea, A. Nica, "The Transient Response of the Electric lines Based on the Equations with Transient Line-Parameters", *Rev. Roum.Sci.Techn.* Vol.23, No.1, pp. 3-19, 1978.
- [16] J. L. Naredo, "The Effect of Corona on Wave Propagation on Transmission Lines", *Ph. D. Dissertation, Electrical Engineering Department, The University of British Columbia*, June, 1992.
- [17] B. Gustavsen and A. Semlyen, "Combined phase domain and modal domain calculation of transmission line transients based on vector fitting." *IEEE Transactions and Power Delivery*, Vol. 13, No. 2, pp. 596-604, Apr. 1998.
- [18] Wedepohl, L.M.; Nguyen, H.V.; Irwin, G.D.; "Frequency-dependent transformation matrices for untransposed transmission lines using Newton-Raphson method", *IEEE Transactions on Power Systems*, Vol. 11, No. 3, pp 1538 - 1546, Aug. 1996.

IX. BIOGRAPHIES

Marisol Dávila C. She received her B.Eng. degree in Electrical Engineering from Universidad de Los Andes, Venezuela in 1993. In 2002 she received the M. Sc. degree from Cinvestav, Guadalajara. She currently is a professor with the Universidad de Los Andes on a leave of absence pursuing the Ph. D. degree at Cinvestav, Guadalajara, México. Her professional interests are in electromagnetic transient analysis and digital protection of power systems.

José Luis Naredo. (IEEE, Senior Member, 2000). He received in 1983 his B.Eng. degree in Mechanical and Electrical Engineering from Universidad Anahuac, México. D. F. In 1987 and in 1992 he obtained, respectively, his M. A. Sc and his Ph.D. degrees, both in Electrical Engineering from the University of British Columbia, Canada. He currently is a full professor with Cinvestav, Guadalajara. His research interests are in electromagnetic transient phenomena and in digital protection and measurements of power systems.

Pablo Moreno V. (IEEE Member, 2001). He received his B. Eng. in Mechanical and Electrical Engineering degree from UNAM, México. D. F. in 1985. He received his M. Sc. degree from ITESM, Monterrey, México, in 1989, and his Ph.D. degree from Washington State University, USA in 1997. He currently is a full professor with Cinvestav, Guadalajara. His research interests are in electromagnetic transients in power systems and in electromagnetic compatibility.